Nucl. Sci. and Tech., Vol.12, No. 1 (2022), pp. 21-31

Nuclear Science and Technology

Journal homepage: http://jnst.vn/index.php/nst

Theoretical consideration of isomeric ratios in some photonuclear reactions induced by bremsstrahlung with endpoint energy in giant dipole resonance region using Talys 1.95 code

Bui Minh Hue[a,b,c] and Tran Duc Thiep[a,b*]

[a]*Graduate University of Science and Technology, VAST, 18 Hoang Quoc Viet, Hanoi 10000, Vietnam*
[b]*Institute of Physics, VAST, 10 Dao Tan St., Ba Dinh Region, Hanoi 10000, Vietnam*
[c]*RIKEN Nishina Center, Wako, Saitama, 351-0198, Japan*
*Corresponding author: tdthiep@iop.vast.vn

Abstract: Isomeric ratios of isomeric pairs produced by photonuclear reactions (γ, n) on Se, Ce, Eu and Hg targets induced by bremsstrahlung with endpoint energies in the giant dipole resonance region have been theoretically calculated using TALYS 1.95 code in combination with Geant4 simulation. The computed isomeric ratios as a function of the bremsstrahlung endpoint energies in the range of 10 to 25 MeV resulted from convolution between calculated differential cross-sections using six level density models available in TALYS 1.95 and the bremsstrahlung spectra simulated by the GEANT4 toolkit. Moreover, for each level density model, eight gamma strength functions have been employed. The calculated results are compared to the experimental data in the existing literature for Talys 1.95 model evaluation.

Keywords: *Isomeric Ratios, (γ, n) reaction, GDR region, Bremsstrahlung, TALYS 1.95 code, GEANT4*

I. INTRODUCTION

The isomeric ratio (IR) furnishes valuable information about the nuclear structure, namely the nuclear level structure and level density of the excited nucleus as well as the nuclear reaction mechanism involved. In practice, the IR can be obtained with high accuracy since the pair of isomers are formed simultaneously during the nuclear reaction process in the same experimental conditions. Therefore, the IRs can be used as precious data for examining different nuclear reaction models. So far, a large number of isomeric ratios have been investigated in almost unlimited nuclear reaction types induced by different projectiles such as photons, neutrons, proton [1- 4], tritium, alpha, heavy ions [5-7], fission products [8], nucleon transfer and complete and incomplete fusion reactions [9]. The theoretical calculation basis of the IR is various nuclear reaction models. Since the 1960s, the well-known statistical model of Huizenga and Vandenbosch [10] has been applied to consider the IR in nuclear reactions induced by various projectiles and led to interesting conclusions about the nuclear structure and reaction mechanisms. The main disadvantage of this model is that the IR strongly depends on the number of gamma rays in the transition cascade. Recently, the TALYS code [11] is a nuclear reaction modeling code employed most often for simulating nuclear reactions and calculating cross-section as well as isomeric ratios. This code simulates nuclear

https://doi.org/10.53747/nst.v12i1.373
Received 31 May 2022, accepted 12 July 2022

reactions induced by neutron, gamma, proton, deuteron, triton, helium-3, and α particle on target nuclei with masses greater than and equal to 12 in the 1 keV-200 MeV energy range. The code considers different nuclear reaction models, i.e., the optical, compound nucleus, pre-equilibrium, direct reaction, fission, and the problems connected to level density and γ-ray strength functions [11]. TALYS uses a database of nuclear structure parameters based on the IAEA Reference Input Parameter Library which provides validated nuclear-model input parameters. However, until now, the IRs in photonuclear reactions are mainly induced by bremsstrahlung. Hence, the TALYS code is often combined with the bremsstrahlung spectra simulated by transportation codes. For this aim, GEANT4 [12], which is a toolkit for Monte Carlo simulations, has been used. This toolkit provides all functionality needed to simulate the detector system, including the interactions of particles, the geometry of the detector system, and the detector response. GEANT4 is a freely available object-oriented software package based on C++, where users build their own simulation applications based upon existing virtual classes.

In this work, we theoretically considered our experimental IR data [13 - 18] and that of Yu. Gangrsky [19], N. Tsoneva [20], A. Belov [21] and A. Tonchev [22] on Se, Ce, Eu, and Hg targets, which have been obtained in the same experimental conditions at electron accelerator Microtron MT-25, JINR Dubna, Russia.

II. CALCULATION PROCEDURE

In this work, the IRs were theoretically calculated by the formula below:

$$IR = \frac{N_0 \int_{E_{th}^m}^{E_\gamma^m} \sigma_m(E)\phi(E)dE}{N_0 \int_{E_{th}^g}^{E_\gamma^m} \sigma_g(E)\phi(E)dE} \quad (1)$$

where E_γ^m - the bremsstrahlung end-point energy, ϕ(E) – the bremsstrahlung photon flux, N_0 - the number of the target nuclei; $\sigma_m(E)$ and $\sigma_g(E)$ – the isomeric-state and ground-state cross sections; E_{th}^m and E_{th}^g - the threshold reaction energies for the isomeric and ground states, respectively.

The formula (1) is applied to all isomeric pairs of interest except for ^{73m,g}Se pair, where IR is calculated as the ratio of the yield of a high spin state to that of a low spin one corresponding to the experimental data.

The flux distribution as a function of bremsstrahlung energies ϕ(E) was obtained by the simulation using the GEANT4 toolkit [11]. This distribution was then convoluted with the theoretical cross-section data $\sigma_m(E)$ and $\sigma_g(E)$ calculated by the TALYS 1.95 code, yielding the theoretical IRs. To investigate IRs depending on various level density models, we changed six level density models available in TALYS 1.95 one by one including 3 phenomenological level density models (Ld1, Ld2 and Ld3) and 3 microscopic level density models (Ld4, Ld5 and Ld6) as follows:

1. Ld1 - Constant Temperature Model + Fermi gas model: In this model, the excitation energy range is divided into one low energy part from E0 up to a matching energy EM, where the so-called constant temperature law is applied and another high energy part above, where the Fermi gas model is applied; 2. Ld2 - Back-shifted Fermi gas Model, in which the pairing energy is treated as an adjustable parameter and the Fermi gas expression is used, 3. Ld3 – Generalized Superfluid Model: In this model, the calculation databases use nuclear structure properties in microscopic level densities based on the deformed Hartree - Fock model; 4. Ld4 - MLD (Skyrme Force) from Goriely's table: In

this model, Goriely's table matching to the Skyrme force, used for calculating microscopic level densities from drip line to drip line on the basis of Hartree-Fock calculations.; 5. Ld5 - MLD (Skyrme Force) from Hilaire's combinational table: In this model, Hilaire's table combinatorial model matching the Skyrme force (HFM) includes a detailed microscopic calculation of the intrinsic state density and collective enhancement; 6. Ld6 - MLD (temperature dependent HFB, Gogny force) from Hilaire's combinational table: In this model, Hilaire's table combinatorial model matching to the Gogny force and is dependent on temperature.

In nuclear reactions, in addition to the level density, the gamma strength function representing the distribution of the average gamma transition probability is also a crucial ingredient to predict the reaction cross-sections. Thus, for each Ld model, we employed eight gamma strength functions available in TALYS 1.95 [11] as input parameters to obtain the cross-sections of isomers, namely: 1. s1- Kopecky-Uhl generalized Lorentzian model is the generalized Lorentzian model (GLO) of Kopecky and Uhl applied for E1 radiation. In this model, the width of gamma transition E1 depends on energy and temperature; 2. s2- Brink-Axel Lorentzian model is standard Lorentzian one (SLO). This is the model implementing the Brink-Axel hypothesis and is widely used to describe the giant electric dipole resonance strength; 3. s3- Hartree-Fock BCS table. This is a microscopic model for E1 radiation. Goriely and Khan calculated gamma-ray strength functions according to the Hartree-Fock Bardeen-Cooper-Schrieffer (HF-BCS) model with Quasiparticle Random Phase Approximation (QRPA) and stored them as tables; 4. s4- Hartree-Fock-Bogolyubov table. This is also a microscopic option calculated by Goriely using Hartree-Fock-Bogolyubov (HFB) model with QRPA; 5. s5- Goriely's hybrid model. This is a Lorentzian model with energy and temperature-dependent width which results in a different type of functional form at low energy than that of Kopecky-Uhl; 6. s6- Goriely T-dependent HFB. In this model, Goriely extended the temperature dependence of HFB model with QRPA; 7. s7- T-dependent RMF. This is the temperature-dependent relativistic mean field model calculated by Daoutidis and Goriely; 8. s8- Gogny DIM HFB+QRPA. This is HFB model with QRPA calculated by Goriely based on the D1M version of the Gogny force.

III. RESULTS AND DISCUSSION

A. The bremsstrahlung photon flux

To simulate as close as possible the experimental condition including geometry and materials of the setup, the primary electron beam, all possible interactions and radiations were described by using GEANT4 leading to a realistic description of the flux distribution. The bremsstrahlung spectra used for photonuclear reactions in the GDR region have been calculated for the end-point energies from 10 to 25 MeV. The simulations were made for the same conditions of our experimental data and that of Yu. Gangrsky [19], N. Tsoneva [20], A. Belov [21] and A. Tonchev [22], which have been all performed on Microtron MT25 as described in ref. [26]. Fig. 1 presents the bremsstrahlung spectra calculated by the Geant4.10.06 version.

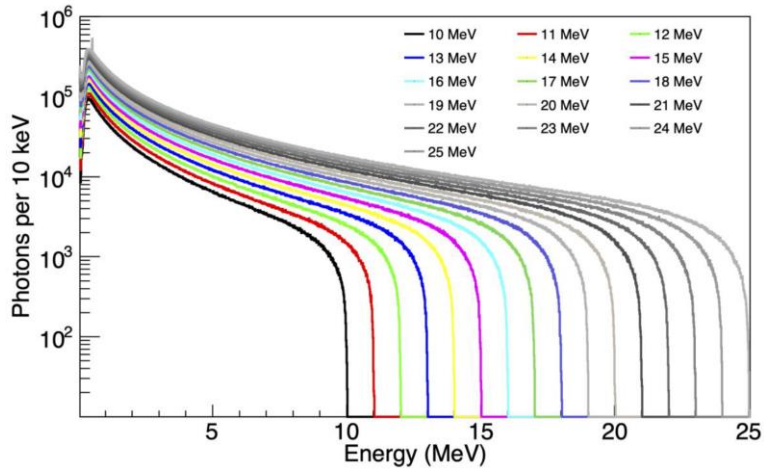

Fig. 1. The bremsstrahlung spectra calculated by Geant4.10.06 version

B. The IRs in photonuclear reactions calculated by Talys code

1. The isomeric, ground state and total cross sections

The cross-sections of the isomeric and ground states $\sigma_m(E)$ and $\sigma_g(E)$ have been calculated with the six level density models and in every model, eight gamma strength functions have been employed as mentioned above. For a typical example, Fig 2 illustrates the cross-sections of isomeric and ground states of ^{137}Ce and ^{152}Eu nuclei, calculated with the level density Ld1 and the gamma strength function s2.

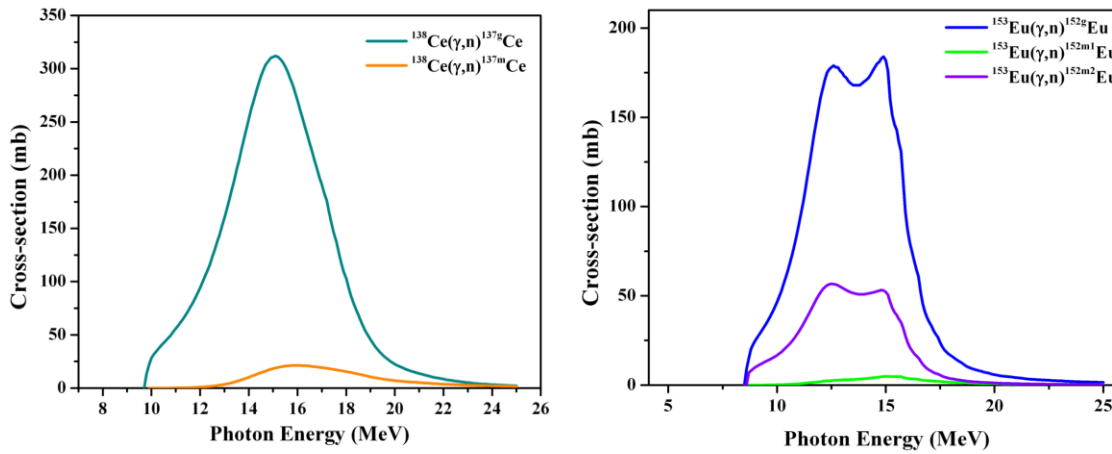

Fig. 2. The calculated cross sections of the isomeric and ground states of ^{137}Ce and ^{152}Eu nuclei

Besides, the total, direct, preequilibrium, and compound reaction cross-sections of the (γ, n) reactions were also calculated to estimate the contributions of these processes. Fig. 3, for example, presents the cross sections for ^{82}Se and ^{198}Hg nuclei. The results show that all investigated nuclei are spherical except for ^{152}Eu being a strongly deformed nucleus as its GDR curve has two maximums (see Fig. 2). The calculations reveal that the compound reaction is dominant in the whole energy range from the reaction threshold to 25 MeV, while the preequilibrium reactions started taking place from 20.3, 16, 17.3, 16.7, 14.9, 15.8 and 15.3 MeV for ^{73}Se, ^{81}Se, ^{137}Ce, ^{139}Ce, ^{152}Eu, ^{195}Hg and ^{197}Hg, respectively. In the case of ^{73,81}Se, the contributions of the direct, preequilibrium, and compound mechanisms are 0%, 3.59%, 96.4%

and 0%, 9.89%, 90.1%, respectively. For ^{137,139}Ce, those are 0%, 2.41%, 97.6% and 0%, 2.88%, 97.1%, respectively. For ^{152}Eu, those are 0%, 6.5%, 93.5%, respectively. For ^{195,197}Hg, those are 0%, 2.0%, 98.0% and 0%, 2.45%, 97.5%, respectively.

The calculated theoretical and the experimental IRs are shown in Figs. 4 to 10. From the obtained results, it is worth making the following remarks:

2. General trend of the dependence of IR on energy

It is seen in Figs from 4 to 10 that there is a general trend of the dependence of calculated IRs on energy similar to the experimental data, namely the IRs for ^{73,81m,g}Se, ^{137,139m,g}Ce, ^{152m1,m2}Eu, ^{195m,g}Hg and ^{197m,g}Hg increase with increasing energy. This fact is reasonable by taking formula (1) into account. One can see from this formula that for the case of photonuclear reaction with bremsstrahlung in the GDR region, the IR increases (or decreases) with the increasing of end-point energy, reaching maximum (or minimum) value at the end of this region and slightly changes for higher energies. The change of IR depends on the yield of the isomeric state increases faster or slower than that of the ground state when the bremsstrahlung end-point energy increases.

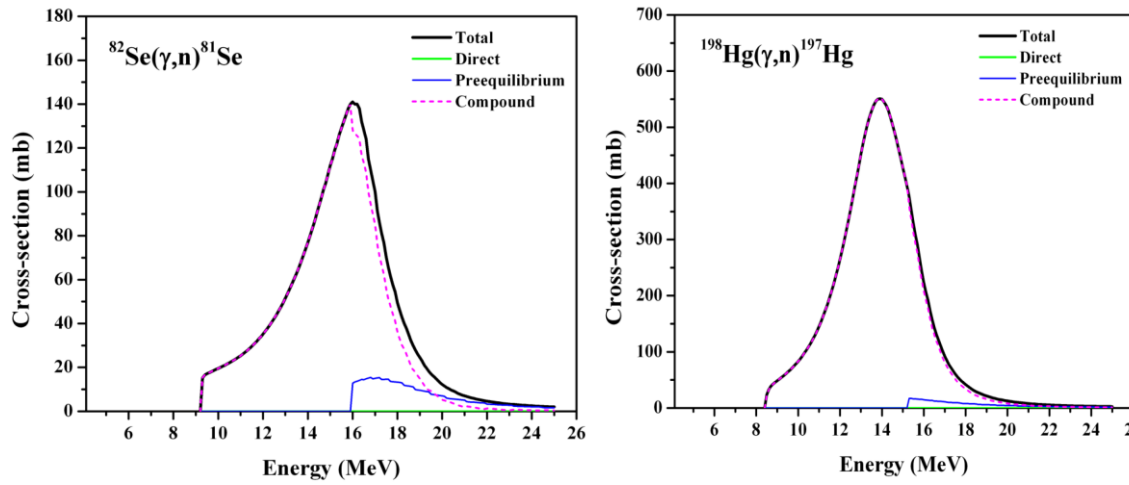

Fig. 3. The direct, preequilibrium, compound and total cross sections of (γ, n) reaction on ^{82}Se and ^{198}Hg, calculated with the level density Ld1 and the gamma ray strength function s2

3. IRs in photonuclear reactions on isotopes

a. For Se isotopes

From Fig. 4, it is seen that the IRs of 73m,gSe calculated by TALYS 1.95 code is not a good description of the experimental data taken from T. D. Thiep [13]. Meanwhile, for 81m,gSe, the calculated IRs excellently describe the experimental data, taken from refs. A. Tonchev [22], B. M. Hue [14] and Yu. P. Gangrsky [19] (see Fig 5). It is worth noting that the best agreements between the experimental and theoretically calculated data for 81m,gSe are Ld1 and Ld2 - models with eight gamma strength functions, Ld4-model with s1 and s7, Ld5-model with s1, s2 and s7 and Ld6-model with almost gamma strength functions, except for s2 and s7 strength functions.

In refs. [13, 23, 24] we show the so-called effect of nucleon configuration, which means that the IR in (γ, n) reaction in the GDR region for isotopes of an element decreases with the increase of the isotope mass number. In the case of Se, the experimental IRs of 73m,gSe are higher than that in 81m,gSe while the theoretical IRs are inverse. Taking into this fact and the

difference in the experimental and calculated results, one can say that the TALYS code may have to make corrections in the level density as well as the gamma strength function models.

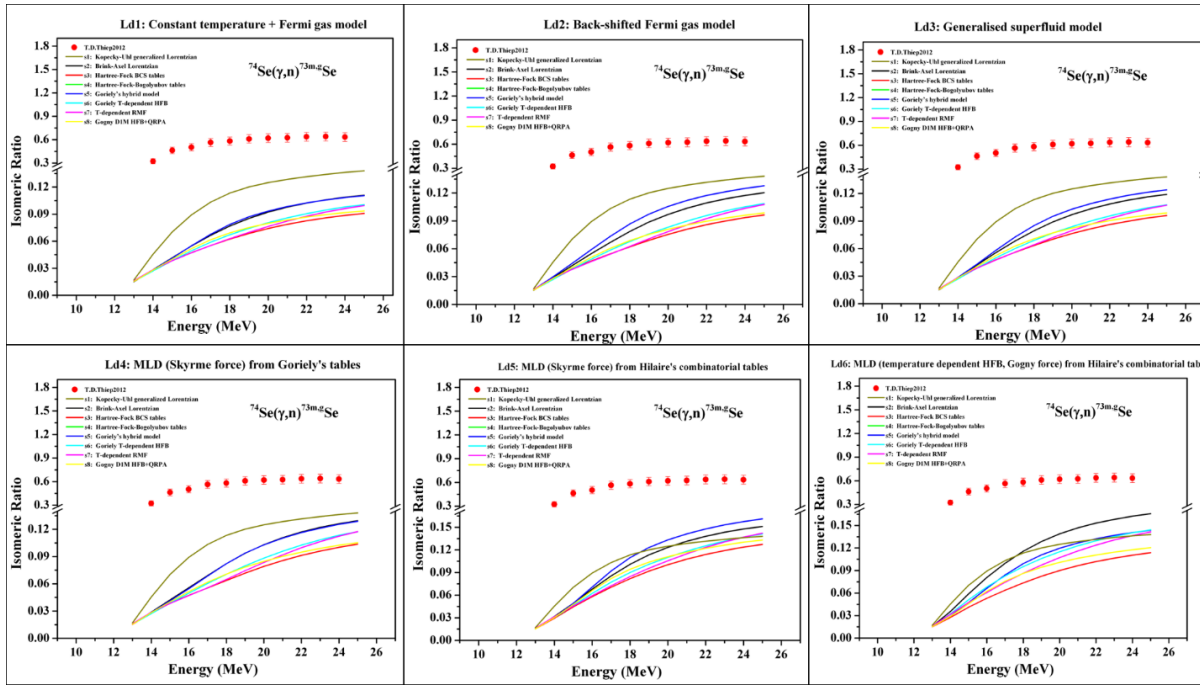

Fig. 4. Experimental and theoretically calculated IRs between ^{73g}Se(I=9/2$^+$) and ^{73m}Se(I=3/2$^-$)

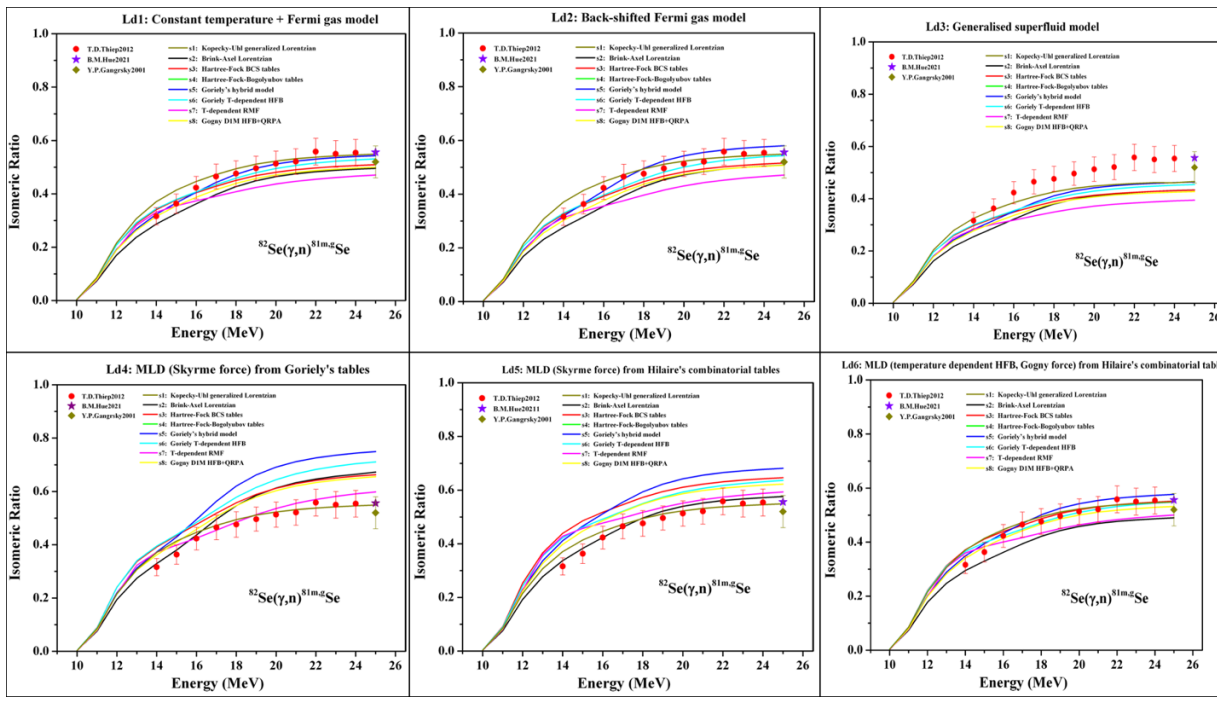

Fig. 5. Experimental and theoretically calculated IRs between ^{81m}Se(I =7/2$^+$) and ^{81g}Se(I=1/2$^-$)

b. For Ce isotopes

Figs. 6 presents the experimental data, taken from B. M. Hue [13], T. D. Thiep [15, 16], Yu. P. Gangrsky [19] and theoretically calculated values for IRs of ^{137m,g}Ce. Fig. 7 presents the experimental data, taken from N. Tsoneva [20], A. G. Belov [21] and theoretically calculated values for isomeric ratios of ^{139m,g}Ce. One can see that for ^{137m,g}Ce there are large deviations between the experimental and theoretical values. On the other hand, for ^{139m,g}Ce, the theoretical calculations well describe the experimental ones, especially the Ld4, Ld5 and Ld6-models. From figs. 6 and 7 one can see that for Ce isotopes, the theoretically calculated data by the Talys code 1.95 also do not show the configuration effect as IRs for ^{137m,g}Ce are lower than that for ^{139m,g}Ce.

c. For Eu Isotopes

The product of (γ, n) photonuclear reaction on ^{153}Eu existed in the ground state with the spin of 3^- and two isomeric states with spins of 0^- and 8^- respectively. Fig. 8 presents the experimental data taken from T. D. Thiep [17, 18] and A. P. Tonchev [22] and theoretically calculated IRs between ^{152m1}Eu(I=8^-) and ^{152m2}Eu(I=0^-). One can see from these figures that there are significant differences between the experimental data and that calculated by six Ld-models with eight gamma strength functions. It is worth noting that ^{153}Eu is a strongly deformed nucleus [25]. In [26] we have incorporated the Talys-calculated differential cross section data into the Geant4 toolkit to proceed with a full simulation of both bremsstrahlung production and photonuclear process as well as to obtain the IRs for Eu isotopes. In this work we employed another method, where only bremsstrahlung spectra obtained from Geant4 code were used to couple with Talys-calculated cross section to calculate the IRs. This method seems more schematic than the full Geant4 simulation in ref. [26], but it should be free from additional bias from the particle transportation involved in Geant4 simulation of photonuclear reaction process. The obtained results from both methods have a good agreement.

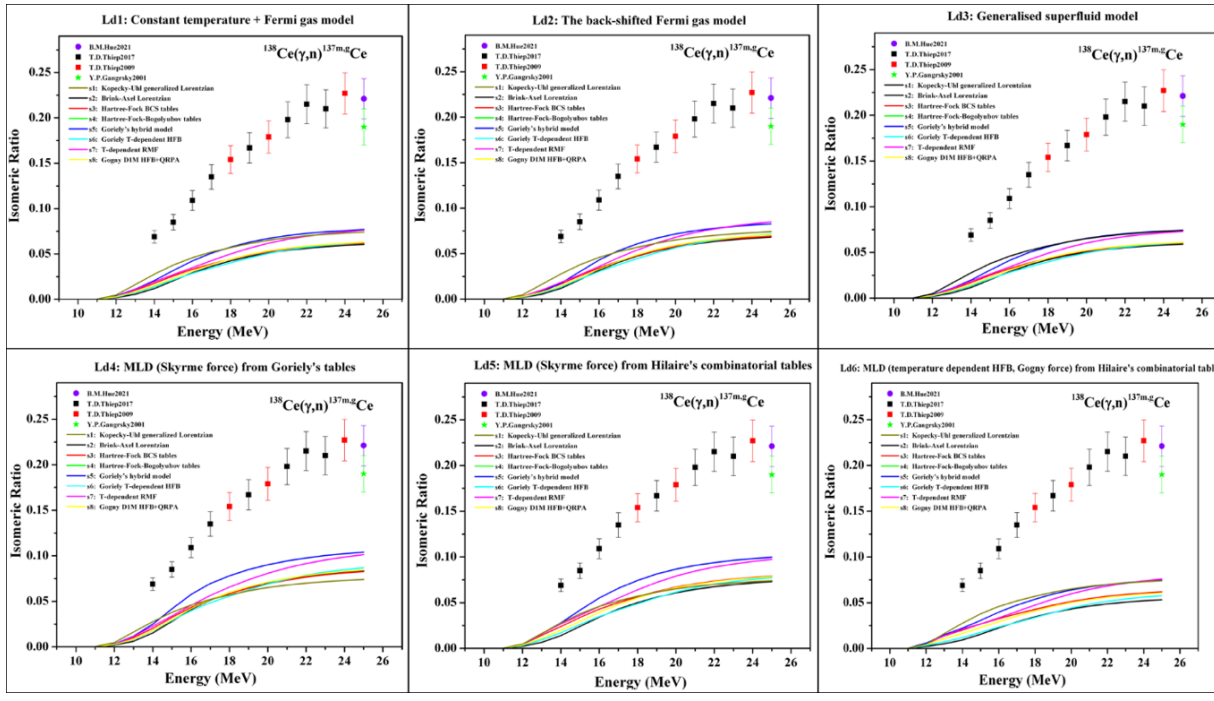

Fig. 6. Experimental and theoretically calculated IRs between ^{137m}Ce(I=$11/2^-$) and ^{137g}Ce(I=$3/2^+$)

d. For Hg isotopes

Fig. 9 presents the experimental data taken from T. D. Thiep [18] and the theoretically calculated IRs between ^{195m}Hg(I=13/2$^+$) and ^{195g}Hg(I=1/2$^-$). Fig. 10 presents the experimental data taken from Yu. P. Gangrsky [19], T. D. Thiep [18] and the theoretically calculated isomeric ratios between ^{197m}Hg(I=13/2$^+$) and ^{197g}Hg(I=1/2$^-$). It is seen that, for ^{195m,g}Hg, six Ld level models relatively well describe the experimental data. In which the six Ld models with s2 – gamma strength function are the best ones, especially LD5 – model with s2. However, for ^{197m,g}Hg, the calculation results are significantly different from the experimental data. It is worth noting that ^{196}Hg and ^{198}Hg nuclei are weakly deformed nuclei [27]. Therefore, this may be a reason that the Talys 1.95 code is unable to show two maximums in the GDR curve (see Fig. 3). It is also noted that the differences between the theoretically calculated IRs and the experimental data for ^{195m,g}Hg and ^{197m,g}Hg are significant. In analogy with the experimental data for Se and Ce isotopes, i.e with the same element, the higher isotope mass number the lower IR, the so-called effect of nucleon configuration [13, 23, 24] can be observed in the experimental IRs for Hg isotopes, namely, the IR of ^{195m,g}Hg are higher than that of ^{197m,g}Hg. The theoretical IR values, calculated by Talys code 1.95 also show this trend similar to that in the experimental data. Therefore, it can be said that for Hg isotopes, the Talys 1.95 code shows the nucleon configuration effect.

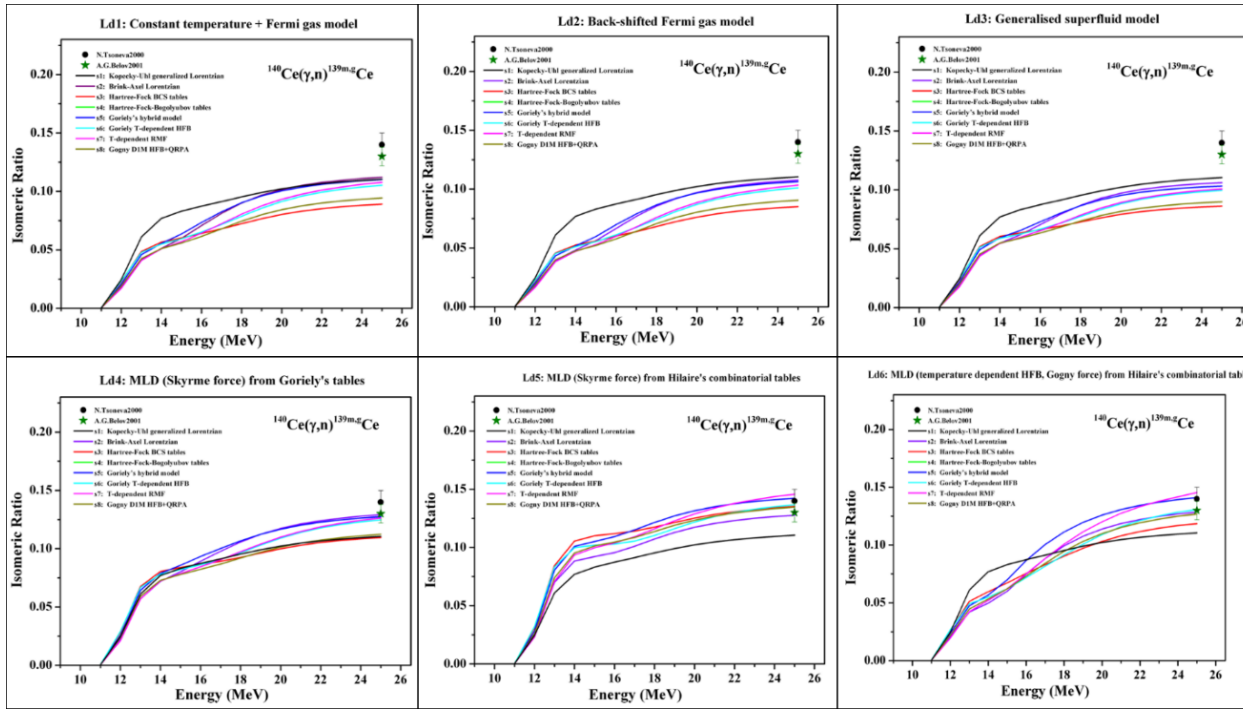

Fig. 7. Experimental and theoretically calculated IRs between ^{139m}Ce(I=11/2$^-$) and ^{139g}Ce(I=3/2$^+$)

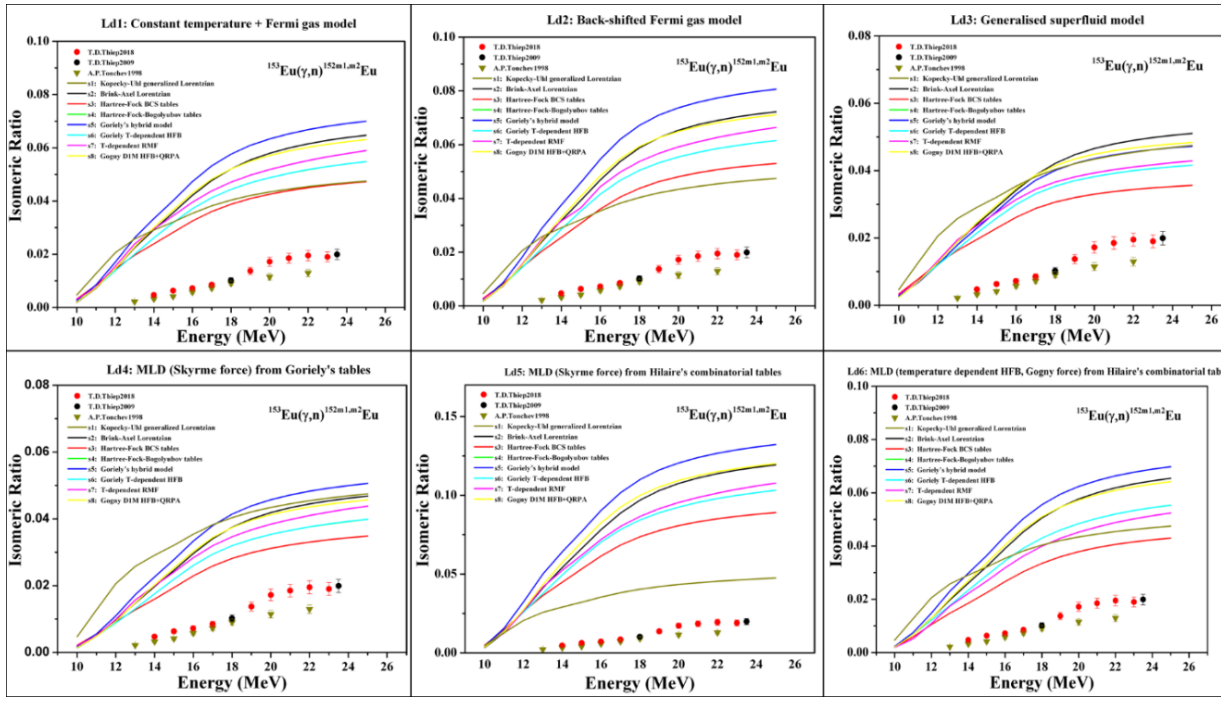

Fig. 8. Experimental and theoretically calculated IRs between ^{152m1}Eu(I=8$^-$) and ^{152m2}Eu(I=0$^-$)

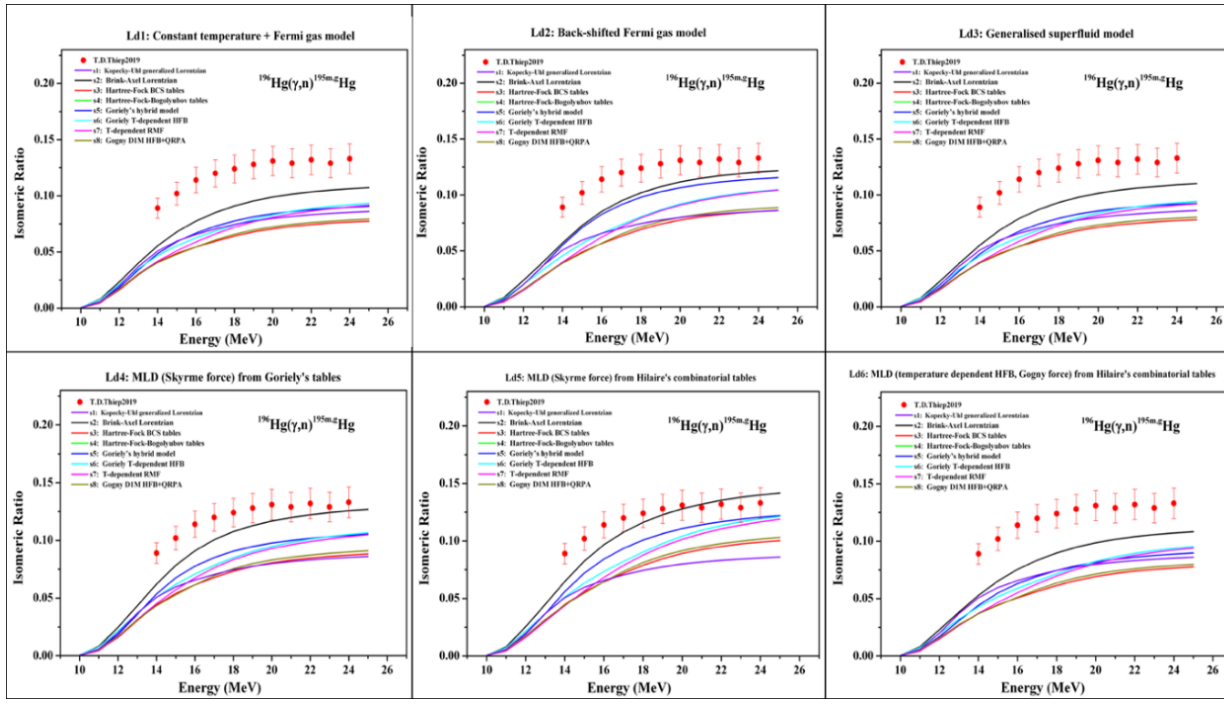

Fig. 9. Experimental and theoretically calculated IRs between ^{195m}Hg(I=13/2$^+$) and ^{195g}Hg(I=1/2$^-$)

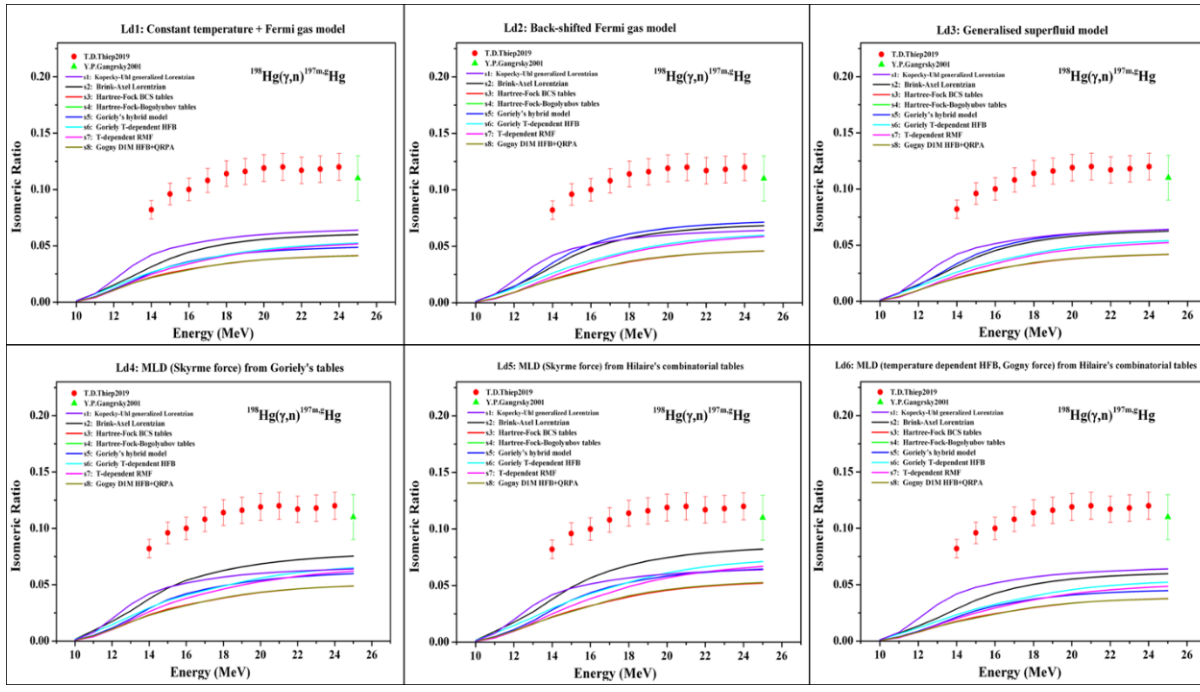

Fig. 10. Experimental and theoretically calculated IRs between ^{197m}Hg(I=13/2$^+$) and ^{197g}Hg(I=1/2$^-$)

IV. CONCLUSIONS

The TALYS 1.95 code in combination with GEANT4 toolkit has been applied to calculate theoretical isomeric ratios in photonuclear reactions (γ, n) in the GDR region on Se, Ce, Eu, Hg targets. The theoretically calculated results were compared to the experimental data in the existing literature. From the results and discussions above, the following preliminary conclusions can be drawn:

- The six Ld models of TALYS 1.95 code well described a general trend in the experimental IRs in photonuclear reactions in the GDR region, namely the IR of the high spin state to that of the low spin state increases with the increase of end-point bremsstrahlung energy for all investigated nuclear reactions.

- The calculations show that the compound reaction is dominant in the whole GDR range, while the preequilibrium reactions started taking place from 20.3, 16, 17.3, 16.7, 14.9, 15.8 and 15.3 MeV for ^{73}Se, ^{81}Se, ^{137}Ce, ^{139}Ce, ^{152}Eu, ^{195}Hg and ^{197}Hg, respectively.

- The TALYS 1.95 code is applicable to calculate the theoretical IR data. In many cases, the results show that the six Ld models with different gamma strength functions well describe the experimental data.

- The six Ld models of TALYS 1.95 code do not show the so-called effect of nucleon configuration in Se and Ce isotopes but show this effect in Hg isotopes.

ACKNOWLEDGMENTS

This work has been performed with financial support from the International Centre of Physics, Institute of Physics under Grant No. ICP.2022.17. Bui Minh Hue was funded by Vingroup JSC and supported by the PhD Scholarship Program of Vingroup Innovation Foundation (VINIF), Institute of Big Data, code VINIF. 2021. TS. 081.

REFERENCES

[1]. Md. S. Rahman, K. Kim, G. Kim, H. Naik, et al, Eur. Phys. J. A, 52, (2016) 194.

[2]. M. Nadeem, M. Zaman, H. Naik, K. Kim, G. Kim, Nuclear Physics A, 970 (2018) 411.

[3]. B. M. Hue, T. D. Thiep, T, T. An, P. V. Cuong, et al, Nucl. Instr. Meth, B, 502 (2021) 46.

[4]. B. Lawriniang, R. Ghosh, S. Badwar, V. Vansola, et al, Nuclear Physics A, 973 (2018) 79.

[5]. M. Ismail, R. P. Sharma, M. H. Rashid, Phys. Rev. C, 57(3) (1998).

[6]. B. Satheesh, M. M. Musthafa, B. P. Singh, et al, Inter. J. Mod. Phys. E, 21(6) (2012) 1250059.

[7]. J. M. Dauga, R. Grzywacz, J. C. Angelique, et al, Phys. Rev. C, 63 (2001) 064609.

[8]. S. Okumura, T. Kawano, P. Jaffke, P. Talou, S. Chiba, J. Nucl. Sci. Tech., 55(9) (2018) 1009.

[9]. G. S. Li, Y. D. Fang, A. Diaz-Torres, M. L. Liu, et al, Phys. Rev. C, 99 (2019) 054617.

[10]. J. R. Huizenga, R. Vandenbosch, Phys Rev, 120 (1960) 1305 and 120 (1960) 1313.

[11]. TALYS 1.95 manual. See also on: https://tendl.web.psi.ch/tendl_2021/talys.html

[12]. GEANT4 toolkit: http://geant4.web.cern.ch

[13]. T. D. Thiep, T. T. An, P. V. Cuong, et al, J. Radioanal. Nucl. Chem. 292(3) (2012) 1035.

[14]. B. M. Hue, T. D. Thiep, Proc. 28th Inter. Sem. on Interaction of Neutrons with Nuclei, Link: http://isinn.jinr.ru/proceedings/isinn-28.html, (2021).

[15]. T. D. Thiep, T. T. An, N. T. Khai, et al, Phys. Part. Nucl. Lett., 6(2) (2009) 126.

[16]. T. D. Thiep, T. T. An, N. T. Khai, et al J. Radioanal. Nucl. Chem., 311(1) (2017) 887.

[17]. T. D. Thiep, T. T. An, N. T. Khai, et al, J. Radioanal. Nucl. Chem., 317 (2018) 1263.

[18]. T. D. Thiep, T. T. An, N. T. Vinh, P. V. Cuong, et al, Nucl. Inst. Meth. B, 457 (2019) 4.

[19]. Yu. P. Gangrsky, P. Zuzaan, N. N. Kolesnikov, et al, Bull. Rus. Ac. Sci. Phys.65 (2001) 121.

[20]. N. Tsoneva, Ch. Stoyanov, Yu. P. Gangrsky, et al, AIP Conf. Proc., 529 (2000) 753.

[21]. A. G. Belov, Yu. P. Gangrsky, L. M. Melnikova, et al, Phys. At. Nucl. 64 (2001) 1901.

[22]. A. P. Tonchev, Yu. P. Gangrsky, A. G. Belov, V. E. Zhuchko, Phys. Rev. C, 58 (1998).

[23]. T. D. Thiep, N. N. Son, T. T. An, N. T. Khai, Comm. in Phys. V. 4, N. 3 (1994) 97.

[24]. T. D. Thiep, T. T. An, P. V. Cuong, N. T. Vinh, J. Radioanal. Nucl. Chem. 292 (2012) 89.

[25]. P. Marmier, E. Sheldon, Book: Phys. Nucl. Part., Acad. Press, New York - London, 1970.

[26]. P. V. Cuong, T. D Thiep, L. T. Anh, Nucl. Inst. Meth. B, 479 (2020), 68.

[27]. K. Shibata, T. Fukahori, S. Chiba, N. Yamamuro, Nucl. Sci. Tech., 34(12) (1997) 1171.